P-29

The effect of fibre length on cement/fibre integration and mechanical properties of a DCPD/PLCL injectable composite biomaterial

John Duckworth[1], Mitsugu Todo[2]

[1]*Interdisciplinary Graduate School of Engineering, Kyushu University*

[2]*Research Institute for Applied Mechanics, Kyushu University*

Abstract

The effect of fibre length in a cement/fibre composite biomaterial on cement/fibre integration, ultimate compressive strength and compressive elastic modulus was investigated. Dicalcium phosphate dihydrate/ poly(lactide-co-ε-caprolactone) 75:25 was the composite material investigated, at a 25%w/w ratio.

A direct relationship between increased fibre length and increasing void volume in the material was determined using micro-CT imaging and Finite Element modelling, attributed to entanglement of the fibres causing poor cement/fibre integration. This in turn was used to explain a measured decrease in the compressive strength of composites with longer fibres, from 32±2 MPa to 24±3 MPa for composites containing 400±100 μm to 1280±350 μm length fibres respectively. It was also found that the compressive elastic modulus of all cement/fibre composites was far lower than that of blank cement alone, from 1.3±0.2 GPa to 270±70 MPa. However, no correlation could be drawn between compressive elastic modulus and void volume or fibre length, as any fibre presence at the set weight ratio had a similar effect.

1. Introduction

Dicalcium phosphate dihydrate (DCPD) is a promising material for use as a bioresorbable, injectable bone cement in a wide range of orthopedic surgeries. An anhydrous mix of precursor reactants, such as β-tri calcium phosphate (β-TCP) and monocalcium phosphate monohydrate (MCPM) in glycerol can be stored indefinitely in liquid form. Upon exposure to aqueous, physiological conditions, as upon injection, a reaction occurs to form the hard, bone-like DCPD cement.

Whilst bone-like in mineral content, the mechanical properties of DCPD cements are very sensitive to preparatory conditions, and in general have yet to be made rugged enough to allow medical application. DCPD has a compressive strength of 10-20 MPa depending on powder/liquid ratios and other environmental effects [1,2]. This is at the low end of known cancellous bone strengths and far below cortical bone strengths [3,4]. Importantly, the compressive elastic modulus of DCPD cement, at around 1-10 GPa, is far higher than that of either cortical or cancellous bone at around 100 MPa and 50 MPa respectively [2,5]. This stiffness differential along with low compressive strength causes significant failure of the cement in any *in vivo* situation.

In an attempt to improve these properties, researchers have incorporated fibres into the cement matrix [6]. One promising material, which has been underinvestigated in this capacity, is poly(lactide-co-ε-caprolactone) 75:25 (PLCL 75:25). The material is known to be bioresorbable, non-toxic and promoting of cell proliferation, and is already in use in other bioresorbable implant technologies available commercially. Its low compressive elastic modulus of 14.2 MPa also allows a more flexible composite, more closely aligned with that of bone [7].

Mean fibre length and cement/fibre integration are known to be key factors in determining the material properties of any such composite material, as they can determine how the cement transfers shear loads and resists fracturing [6,8]. For PLCL containing composites, this is even more

important, as the hydrophobic nature of the material often prevents strong cement/fibre integration. Micro-scale, x-ray computer tomography (micro-CT) has previously been used as a tool to map fibre distribution and cement/fibre integration within a given sample in medical engineering [9].

2. Methods

This study uses PLCL fibres in a DCPD cement matrix to investigate these relationships on a macro scale.

2.1 DCPD cement/PLCL fibre composite

Monocalcium phosphate monohydrate (Sigma Aldrich, #BCBP5940V, USA) was combined with β-tricalcium phosphate (Taihei Chemicals Ltd., #09090301, Japan) in a 1:1 molar ratio to form the dry powder as suggested by Han et al. [10]. This was in turn combined with glycerol (Sigma Aldrich, #SHBG8251V, USA) in a solid/liquid mass ratio of 3.7, to form the anhydrous slurry.

Raw PLCL fibres were formed using a commercial melt-spinner (EAST, EA-WA2805, Japan) by heating PLCL 75:25 pellets (Gunze Ltd., Japan) to 155˚C under high rotation. The resulting fibre mats were further processed to create four distinct loose fibres of varying length and length distribution. Fibre Type A was fresh PLCL, manually shredded. Fibre Type B was fresh PLCL shredded into loose fibres using a mechanical rotary cutter. Type C and D fibres were formed from PLCL aged in a humid atmosphere for 3 months to degrade the floss by hydrolysis. Type C was then manually shredded, whilst Type D used the mechanical rotary cutter. In all instances, *n=10*. Fibre lengths were determined visually, using a field-emission scanning electron microscope (FE-SEM) (Hitachi Ltd., S-4100, Japan).

Anhydrous cement slurries were combined with PLCL fibres at 25%w/w ratio and mechanically mixed with a spatula for >5 minutes. This final slurry was compressed into a Teflon mold using a spatula and Teflon rod. Samples were then incubated in phosphate buffer solution (PBS) (Wako Chem., Japan) under 5% CO_2 at 37˚C for 48 hours to simulate physiological conditions post-injection.

2.2 X-ray Diffractometry

X-ray diffractometry (XRD) was performed using filtered CuK-α radiation generated at 30kV and 15mA using a Rigaku MiniFlex II Tabletop XRD (Rigaku, Japan) x-ray diffractometer. Each of the five samples as well as samples of each reactant and the product of the reaction were detected. This was done in order to confirm the completion of the reaction, and determine whether the fibre length present in samples prevented completion.

2.3 Micro-CT imaging

A Bruker SKYSCAN 1176 – High Resolution X-Ray Microtomograph (Bruker, Belgium) was used to image samples of cement containing each fibre type, alongside a blank control. Images were taken using a 0.5mm aluminium filter at 50kV and 500μA current. The resulting images were accurate to a scale of 8.8μm. The software Mechanical Finder v7.0 was used to stitch individual images into three-dimensional Finite Element (FE) models for analysis.

2.4 Determining Cement/Fibre Integration

From the FE models, the external volume, V_E was determined. This is the volume assuming the sample has no voids or fibre content within. Then, the true volume, V_T was determined. The difference between the two, minus the fibre volume, V_F, gives the volume of voids, V_S. The ratio of V_S/V_E provides a dimensionless parameter for cement/fibre integration. Equation 1 summarizes this calculation.

$$V_S / V_E = (V_E - (V_T + V_F)) / V_E \quad \text{(Eq.1)}$$

2.5 Mechanical Testing

The compressive elastic modulus of each sample was determined via compression tests using a Shimadzu EZ-S Compact Tabletop Testing

P-29

Machine (Shimadzu, Japan). A flat crosshead and baseplate were used with a crosshead speed of 1mm/min and a 500N load cell. The region under measurement was 5mm in radius and of thickness measured *in situ*. Samples were tested wet, directly after removal from PBS.

Compressive strength testing was performed using the same Shimadzu EZ-S Compact Tabletop Testing Machine (Shimadzu, Japan) with a steel 45˚ wedge crosshead against a flat baseplate at 1mm/min crosshead speed with a 100N load cell. Samples were tested wet, directly after removal from PBS.

3. Results

3.1 Mean Fibre Length

The results from the FE-SEM imaging are summarized in Table 1, establishing the variation in fibre length from the four processing methods.

Table 1: Variation in mean fibre length and distribution of length for each processing method.

Label	Mean Fibre Length / µm	σ / µm	n
Type A	1280	350	10
Type B	416	107	20
Type C	744	238	16
Type D	445	127	20

3.2 X-Ray Diffractometry

Figure 1 gives the XRD summary of each sample. All cement/fibre composites showed 2θ peaks at 11.8 and 21.1, indicating DCPD present. All also showed no 2θ peaks at 15.2 and 46.6, indicating no significant MCPM present, hence a completed reaction. 2θ peaks at 27.9, 31.1 and 34.4 are attributed to excess β-TCP.

3.3 Micro-CT Images and Void Calculation

V_E and V_T of each sample was determined using Mechanical Finder v7.0. Figure 2 visualizes each volume. Figure 3 uses the software data and Equation 1 to calculate the percentage volume of

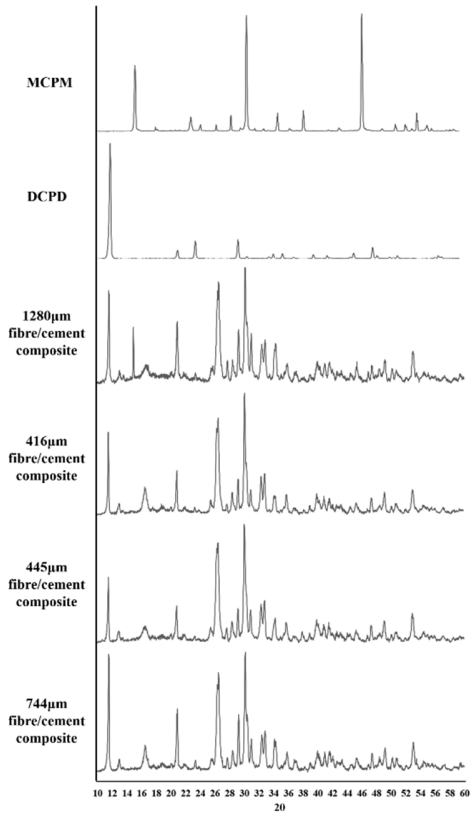

Figure 1: XRD data showing conversion of MCPM to DCPD in all four cement/fibre samples.

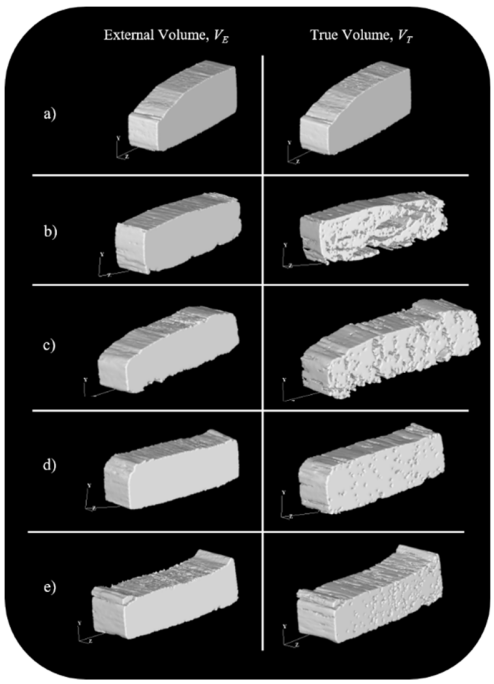

Figure 2: Fig 1: FE models from micro CT showing V_E and V_T of a) blank DCPD b) 1280, c) 744, d) 445 and e) 416 µm length fibre containing DCPD cement.

void space in cement with each fibre length, V_S / V_E. As expected, the percentage volume of voids in blank DCPD cement approached zero, indicating that fibre presence was the major cause of void formation.

Decreasing fibre length correlated linearly to decreasing percentage volume of voids within the composite. Thus, it is accurate to use V_S / V_E, the percentage volume of voids, as a parameter for fibre/cement integration.

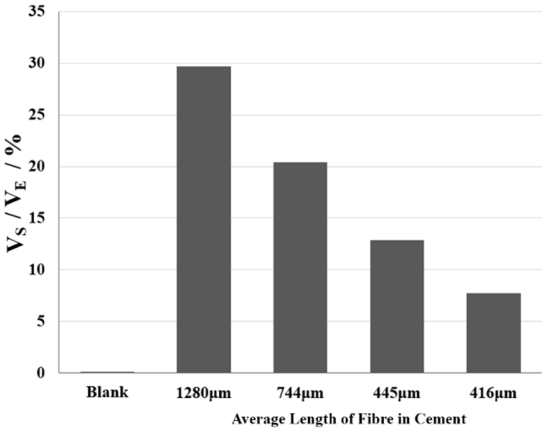

Figure 3: V_S / V_E, for various length fibre containing composites.

3.4 Mechanical Testing

The compressive elastic modulus of DCPD cement was significantly reduced by fibre content of any length, from 1.3±0.2 GPa to 270±70 MPa. Figure 4 shows the reduction in compressive elastic modulus across varying percentage volume of voids, V_S / V_E. It seems that no relationship statistically exists between percentage empty space and compressive elastic modulus, indicating the fibre material itself, or some other variable, is the most important factor for determining compressive elastic modulus.

Figure 5 shows the variation in compressive strength for composites with varying V_S / V_E. Cement containing the fewest voids, at 7.7%v/v, showed the largest increase in compressive strength from the blank cement, from 16±3 MPa to 32±2 MPa. All fibre content increased the compressive strength of the composite

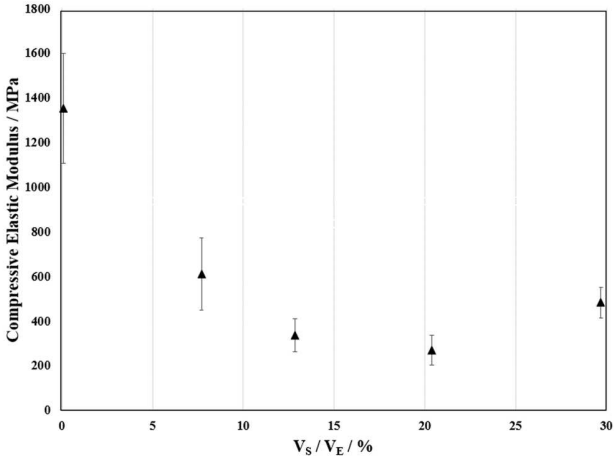

Figure 4: Variation in compressive elastic modulus for DCPD/PLCL cement/fibre composites with increasing percentage volume of voids in the cement, *n=10*.

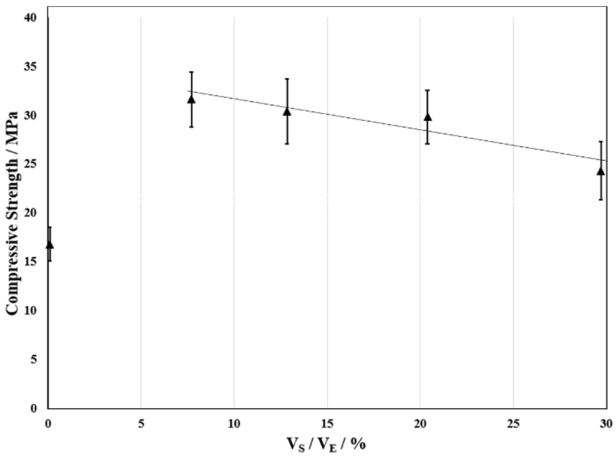

Figure 5: Variation in compressive strength of DCPD cement composites with increasing percentage empty space, *n=10*. Trend shows the relationship between fibre containing cements.

significantly, but increasing V_S / V_E is correlated linearly to decreasing compressive strength. This indicates that fibres that increase the volume of voids in a cement are likely to directly weaken the overall compressive strength of the composite.

4. Discussion

Micro-CT imaging allows us to calculate the percentage volume of voids, V_S, inside a composite material in a completely non-destructive way. It

P-29

was shown that shorter fibres are inversely, linearly correlated to V_S in DCPD/PLCL cement/fibre composites. The hydrophobic nature of PLCL, or natural entanglement could be encouraging longer fibres to resist integration. It has been shown in Figure 5 that the increase in void volume directly weakens the composite, decreasing its compressive strength. The best performing composite materials had void volumes of 7.7%v/v, but lower void volumes with fibre containing composites were not investigated. As the relationship appears to be linear, this suggests even greater compressive strengths than 32±2 MPa are possible, potentially entering ranges where medical applications become possible.

It was also seen that the compressive elastic modulus depends more on the presence of fibres, rather than baring any relationship to the volume of void space within the composite. However, whilst showing no relationship with the volume of voids in the material, DCPD/PLCL composites all showed a greatly reduced compressive elastic modulus, bringing them within the range of cortical and cancellous bone.

5. Conclusion

This study showed that the modern, non-destructive technique of micro-CT imaging can be used to analyse the internal structure of DCPD/PLCL fibre composite materials. It was shown through this method that fibre length correlated linearly to increasing void space in the composite material, and that this has a direct effect on the compressive strength of the material. It was shown that PLCL fibre presence reduced the compressive elastic modulus of the material to within the biological range of cortical and cancellous bone, but held no clear correlation to void volume.

Further reduction of void volume in DCPD/PLCL cements promises to provide stronger composites, whilst the confirmed reduction of compressive elastic modulus gives hope of the material's application in the near future.

6. Acknowledgements

I would like to thank Mitsugu Todo sensei for his support and guidance, as well as Nakamuta San and Aziza Intan San for their technical advice. I would also like to thank Kanji Tsuru sensei and Takaaki Arahira sensei at Fukuoka Dental College for allowing me access to their x-ray laboratory, which made this work possible. I would also like to thank Green Asia for their financial and administrative support.

References

[1] Ginebra MP (2008) Calcium phosphate bone cements. Woodhead Publishing Ltd., Cambridge.
[2] Charriere E, Terrazzoni S, Pittet C, Mordasini Ph, Dutoit M, et al. (2001) Mechanical characterization of brushite and hydroxyapatite cements. Biomaterials 22: 2937-2945.
[3] Carter DR, Hayes WC (1977) The compressive behaviour of bone as a two phase porous structure. Clin Orthop Relat Res 59A: 954-962.
[4] Burstein AH, Reilly DT, Martens M (1977) Aging of bone tissue: mechanical properties. J Bone Joint Surg 58A: 82-86.
[5] Misch CE, Qu Z, Bidez MW (1999) Mechanical properties of trabecular bone in the human mandible: implications for dental implant treatment planning and surgery placement. J Oral Maxillofac Surg 57(6): 700-706.
[6] Canal C, Ginebra MP (2011) Fibre-reinforced calcium phosphate cements: A review. J Mech Behav Biomed 4(8): 1658-1671.
[7] Kwon IK, Kidoaki S, Matsuda T (2005) Electrospun nano- to microfiber fabrics made of biodegradable copolyesters: structural characteristics, mechanical properties and cell adhesion potential. Biomaterials 26(18): 3929-3939.
[8] Lassila LV, Tezvergil A, Lahdenpera M, Alander P, Shinya A, et al. (2005) Evaluation of some properties of two fibre-reinforced composite materials. Acta Odontol Scand 63(4): 196-204.

P-29

[9] Uzun IH, Malkoc MA, Keles A, Ogreten AT (2016) 3D micro-CT analysis of void formations and push-out strength of resin cements used for fiber post cementation. J Adv Prosthodont 8(2): 101-109.
[10] Han B, Ma P, Zhang L, Yin Y, Tao K, et al. (2009) β-TCP/MCPM-based premixed calcium phosphate cements. Acta Biomater 5: 3165-3177.